

Temperature Acceleration of Dielectric Charging in RF MEMS Capacitive Switches

Xiaobin Yuan, *Student Member, IEEE*, Zhen Peng, *Student Member, IEEE*, James C. M. Hwang, *Fellow, IEEE*, David Forehand, *Member, IEEE*, and Charles L. Goldsmith, *Senior Member, IEEE*

Abstract — Temperature acceleration of dielectric-charging effects in state-of-the-art RF MEMS capacitive switches was characterized and modeled. From the measured charging and discharging transient currents at different temperatures, densities and time constants of traps in the dielectric were extracted. It was found that, while charging and discharging time constants are relatively independent of temperature, steady-state charge densities increase with temperature. A charging model was constructed to predict the amount of charge injected into the dielectric and the corresponding shift in actuation voltage under different temperatures. Agreement was obtained between the model prediction and experimental data.

Index Terms — RF, MEMS, switch, dielectric, charging, trap, temperature acceleration.

I. INTRODUCTION

Despite their nearly-ideal high-frequency characteristics, lifetime of electrostatically actuated RF MEMS capacitive switches is limited by dielectric-charging effects [1]. To date, dielectric-charging effects in RF MEMS devices have been studied by different research groups [2]-[4]. We have proposed an approach to characterize the switch dielectric and extracted a charging model to predict charge injection and actuation-voltage shift at room temperature [2]. However, for switch applications in harsh environment (e. g., over the military temperature range of -55 to 125°C), temperature effects on charging also need to be modeled and characterized. In this paper, we present the results on temperature acceleration of the dielectric-charging effects in state-of-the-art RF MEMS capacitive switches. By using the methodology proposed in [2], a temperature-dependent charging model was extracted to

predict the actuation-voltage shift under different temperatures and found to be in agreement with the experimental data.

II. EXPERIMENTAL

The device under study is a state-of-the-art metal-dielectric-metal RF MEMS capacitive switch fabricated on a glass substrate [2]. The dielectric is sputtered silicon dioxide with a thickness of $0.25\ \mu\text{m}$ and a dielectric constant of 4.5. The top electrode is a $0.3\text{-}\mu\text{m}$ -thick flexible aluminum membrane that is grounded. The bottom chromium/gold electrode serves as the center conductor of a $50\ \Omega$ coplanar waveguide for the RF signal. Without any electrostatic force, the membrane is normally suspended in air $2.5\ \mu\text{m}$ above the dielectric. Control voltage with a magnitude of $25\text{-}35\ \text{V}$ is applied to the bottom electrode, which brings the membrane in contact with the dielectric thus forming a $120\ \mu\text{m} \times 80\ \mu\text{m}$ capacitor. The dielectric-charging effect was studied by applying a $-30\ \text{V}$ stress voltage on the bottom electrode of the switch for different time periods under different temperatures while measuring the corresponding actuation-voltage shifts.

In order to extract the temperature-dependent charging model, charging and discharging transient currents [2] were measured under different temperatures on a $500\ \mu\text{m} \times 500\ \mu\text{m}$ metal-insulator-metal (MIM) capacitor with the same electrode and dielectric materials as the switch. A precision semiconductor parameter analyzer (Agilent 4156C) was used to force a $-30\ \text{V}$ pulse on the bottom electrode of the MIM capacitor while sensing the transient current. Well-guarded probe station and probes were used to suppress the capacitive and leakage currents in the measurement path, thus extending the transient current measurement range below pA level.

When a voltage pulse is applied to the MIM capacitor, the total current across the capacitor includes displacement current, trap charging current, and steady-state leakage current. Since the time constant for the displacement current is of the order of milliseconds, the transient currents measured in seconds comprise mainly trap charging currents. Similarly, transient currents measured after the voltage pulse is removed comprise mainly trap discharging currents [2]. This way, trap

Manuscript submitted on March 10, 2006. Work was partially supported by the US Air Force Research Laboratory under Contract No. F33615-03-C-7003. The contract was funded by the US Defense Advanced Research Projects Agency under the Harsh Environment, Robust Micromachined Technology (HERMIT) program.

X. Yuan, Z. Peng, and J. C. M. Hwang are with Lehigh University, Bethlehem, PA 18015 USA. J. C. M. Hwang can be contacted at (610) 758-5104 or jh00@lehigh.edu.

D. Forehand and C. Goldsmith are with MEMtronics Corp., Plano, TX 75075 USA.

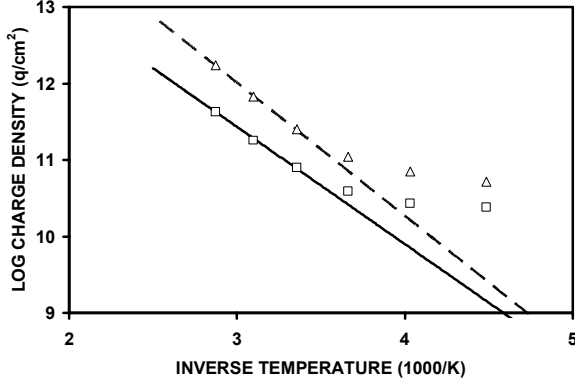


Fig. 1. Comparison of extracted and fitted temperature dependence of steady-state charge densities at -50 , -25 , 0 , 25 , 50 , and 75°C . Extracted steady-state charge densities are for (\square) trap 1 and (Δ) trap 2. Fitted steady-state charge densities are for (—) trap 1 and (---) trap 2.

densities and charging/discharging time constants can be extracted from the measured transient currents at different temperatures.

III. MODEL EXTRACTION

The injected charge density in the dielectric can be modeled as [2]

$$Q = \sum_j Q_j [1 - \exp(-t_{ON} / \tau_{Cj})] \exp(-t_{OFF} / \tau_{Dj}), \quad (1)$$

where Q_j is the steady-state charge density of the J th species of trap, τ_{Cj} and τ_{Dj} are the charging and discharging time constants of the J th species of trap, t_{ON} and t_{OFF} are the on and off times of the switch corresponding to the charging and discharging times.

Assuming all traps are empty before applying the control voltage pulse, transient current after the voltage is turned on is

$$I_C = qA \frac{dQ}{dt} = qA \sum_j \frac{Q_j}{\tau_{Cj}} \exp(-t_{ON} / \tau_{Cj}), \quad (2)$$

where q is the electron charge, and A is the surface area of the dielectric. Similarly, assuming the traps are all charged during the voltage pulse duration, transient current due to the discharging of the traps after removal of the voltage is

$$I_D = qA \frac{dQ}{dt} = -qA \sum_j \frac{Q_j}{\tau_{Dj}} \exp(-t_{OFF} / \tau_{Dj}). \quad (3)$$

Charging model parameters Q_j , τ_{Cj} , and τ_{Dj} were extracted at each temperature (-50 , -25 , 0 , 25 , 50 , and 75°C) by fitting the measured transient currents under -30 V bias with exponential functions of (2) and (3).

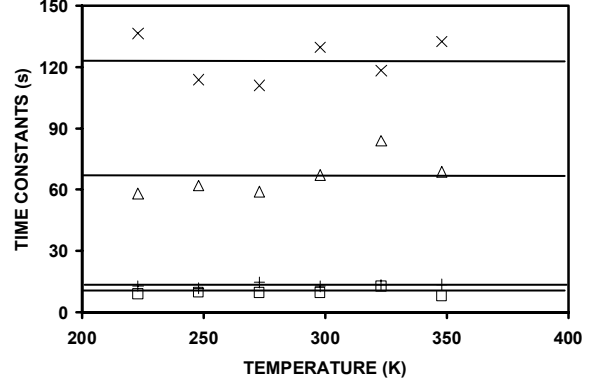


Fig. 2. Extracted (\square) trap 1 charging, ($+$) trap 1 discharging, (Δ) trap 2 charging, and (\times) trap 2 discharging time constants at -50 , -25 , 0 , 25 , 50 , and 75°C . Solid lines indicate the average values of the time constants over temperature.

Two exponential functions, representing two trap species, were found to give good fit.

As shown in Fig. 1, the extracted steady-state charge densities for trap 1 and trap 2 both increase with temperature. Temperature dependence of the steady-state charge density for the J th trap is modeled using the standard equation for a thermally activated process

$$Q_j = Q_{0j} \exp(-E_{Aj} / kT), \quad (4)$$

where Q_0 is a fitting parameter, E_A is the activation energy, k is Boltzmann constant, and T is temperature. By using (4), temperature dependence of the steady-state charge density was fitted reasonably well for temperatures above 0°C as shown in Fig. 1. For temperatures below 0°C , extracted data points deviate from the fitted line indicating that a different process hence a different set of Q_0 and E_A should be considered. Since the steady-state charge density is larger at higher temperatures while the membrane is more prone to stiction (smaller spring constant at higher temperatures), it is more important for the model to be accurate at higher temperatures. Therefore, to reduce the complexity of the model, only one set of Q_0 and E_A were used to give the best fit of the temperature-dependent charge densities above 0°C as shown in Fig. 1.

While the steady-state charge densities are temperature dependent, the extracted charging and discharging time constants are relatively independent of temperature as shown in Fig. 2. Therefore, τ_C and τ_D were taken as the average of the time constants extracted under different temperatures.

From the measured charging and discharging transient currents on the MIM capacitor, charging model parameters were extracted for the -30 V control voltage

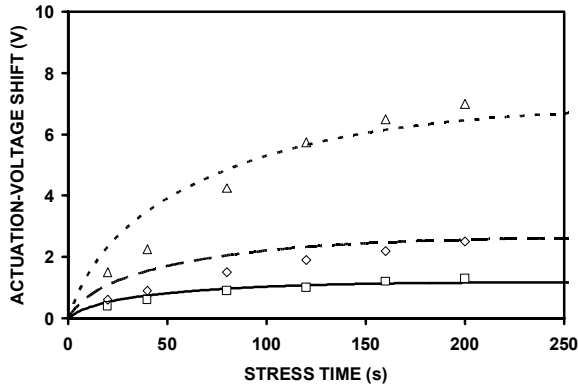


Fig. 3. Measured actuation-voltage shift at (\square) 0, (\diamond) 25, and (Δ) 50°C. Modeled actuation-voltage shift for (—) 0, (---) 25, and (⋯) 50°C. Measurement was taken after 20, 40, 80, 120, 160, and 200 s of -30 V stress on the bottom electrode of the switch. The charge sheet is assumed to be 180 nm away from the bottom switch electrode.

TABLE I
EXTRACTED MODEL PARAMETERS

J	τ_C (s)	τ_D (s)	Q_0 (q/cm ²)	E_a (eV)
1	9.8	13.2	1.07×10^{16}	0.30
2	66.5	123.6	1.71×10^{17}	0.35

as listed in Table I. This charging model was used to predict the actuation-voltage shift under different temperatures.

IV. MODEL VERIFICATION

The dielectric-charging effect on the state-of-the-art RF MEMS capacitive switch was measured by applying a stress voltage on the bottom electrode of the switch for different time periods while measuring the corresponding actuation-voltage shift. The -30 V stress voltage used in the experiment is sufficient to actuate the switch at all measurement temperatures (0, 25, and 50°C). The actuation voltage was shifted in the positive direction (less negative) after the stress indicating injection of electrons from the bottom electrode into the dielectric at all temperatures.

The actuation-voltage shift due to dielectric charging can be expressed as

$$\Delta V = qhQ / \epsilon_0 \epsilon_r, \quad (5)$$

where h is the distance between the bottom electrode and the trapped charge sheet, Q is the injected charge density predicted by (1), ϵ_0 is the permittivity of free space, and ϵ_r is relative dielectric constant of the switch dielectric.

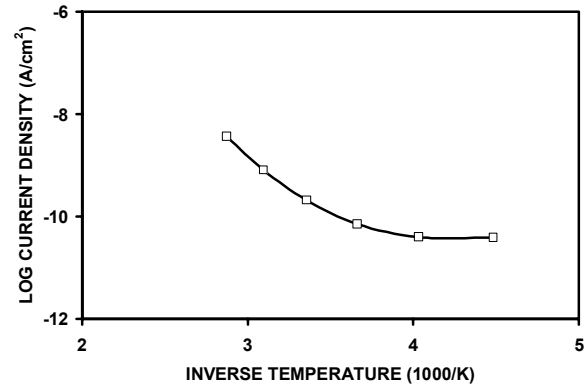


Fig. 4. Measured steady-state leakage current on the $500 \times 500 \mu\text{m}^2$ capacitor under -30 V bias at -50 , -25 , 0 , 25 , 50 , and 75°C .

Since h can not be directly measured, the actuation-voltage shift for a certain stress period is predicted by the charging model (1), (4), and (5) with h optimized to give the best fit between model prediction and experimental data at all temperatures. Fig. 3 shows the measured and modeled actuation-voltage shifts after different stress periods at different temperatures. Agreement was obtained for all temperatures by using $h = 180$ nm, which is approximately two thirds of the dielectric thickness.

V. DISCUSSION

The extracted charging and discharging time constants are independent of temperature. This indicates that the extracted time constants are not capture and emission times for the traps. Instead, the extracted time constants are characteristic of the diffusion-like charge redistribution process within the relatively thick dielectric. Once significant amount of charges are injected from the metal into the dielectric, they alter the field at the interface so that additional injection can occur only after the initial charges have sufficient time to diffuse inside the dielectric by trap hopping. The process is rather complicated and the time constants for the process showed no temperature dependence within our measurement temperature range as shown in Fig. 2. The steady-state charge densities were found to be thermally activated and were modeled using (4). Similar observations have been made on amorphous silicon thin-film transistors [5]-[7].

The injected charges are most likely distributed across the thickness of the dielectric. Since their collective effect on the actuation voltage can be approximated by a charge sheet, it greatly simplifies the model by using the charge-sheet assumption. In addition, the difference

between the MIM capacitor and the actual switch is also absorbed in the h parameter which defines the location of the charge sheet.

For the silicon dioxide used in this study, high leakage current is not necessarily desirable to reduce charge trapping. As shown in Fig. 4, the measured steady-state leakage current increases at elevated temperatures. However, the steady-state charge density and corresponding actuation-voltage shift also increase with temperature as shown in Fig. 1 and 3. Meanwhile, the spring constant and restoring force of the membrane decrease at elevated temperatures; therefore, the switch is more prone to charge-induced stiction when temperature increases. Conversely, lowering the temperature will increase the membrane spring constant while reducing the charge injection, which will render a longer switch lifetime.

VI. CONCLUSION

Temperature acceleration of dielectric-charging effects in state-of-the-art RF MEMS capacitive switches was successfully characterized and modeled. It was found that, while charging and discharging time constants are relatively independent of temperature, steady-state charge densities increase with temperature. A temperature-dependent charging model was constructed to predict the amount of charge injected into the dielectric and the corresponding shift in actuation voltage. Agreement was obtained between the modeled and measured actuation-voltage shift.

REFERENCES

- [1] C. L. Goldsmith, J. Ehmke, A. Malczewski, B. Pillans, S. Eshelman, Z. Yao, J. Brank, and M. Eberly, "Lifetime characterization of capacitive RF MEMS switches," in *IEEE MTT-S Int. Microwave Symp. Dig.*, vol. 1, June 2001, pp. 227-230.
- [2] X. Yuan, J. C. M. Hwang, D. Forehand, and C. L. Goldsmith, "Modeling and characterization of dielectric-charging effects in RF MEMS capacitive switches," in *IEEE MTT-S Int. Microwave Symp. Dig.*, June 2005, pp. 753-756
- [3] J. R. Reid and R. T. Webster, "Measurements of charging in capacitive microelectromechanical switches," *Electron. Lett.*, vol. 38, no. 24, pp. 1544-1545, Nov. 2002.
- [4] W. M. van Spengen, R. Puers, R. Mertens, and I. De Wolf, "A comprehensive model to predict the charging and reliability of capacitive RF MEMS switches," *J. Micromech. Microeng.*, vol. 14, no. 4, pp. 514-521, Jan. 2004.
- [5] S. W. Wright and J. C. Anderson, "Trapping centers in sputtered SiO₂ films," *Thin Solid Films*, vol. 62, pp. 89-96, 1979.
- [6] M. J. Powell, "Charge trapping instabilities in amorphous silicon-silicon nitride thin-film transistors," *Appl. Phys. Lett.*, vol. 43, pp. 597-599, Sep. 1983.
- [7] A. V. Gelatos and J. Kanicki, "Bias stress-induced instabilities in amorphous silicon nitride/hydrogenated amorphous silicon structures: Is the "carrier-induced defect creation" model correct?" *Appl. Phys. Lett.*, vol. 57, pp. 1197-1199, Sep. 1990.